Magnetic flux noise in SQUIDs and qubits

By

Steven Matthew Anton

A dissertation submitted in partial satisfaction of the

requirements for the degree of

Doctor of Philosophy

in

Physics

in the

Graduate Division

of the

University of California, Berkeley

Committee in charge:

Professor John Clarke, Chair
Professor Irfan Siddiqi
Professor Theodore Van Duzer

Spring 2013

Magnetic flux noise in SQUIDs and qubits

Abstract

Magnetic flux noise in SQUIDs and qubits

by

Steven Matthew Anton

Doctor of Philosophy in Physics

University of California, Berkeley

Professor John Clarke, Chair

My work is awesome. Give me a Ph.D.

I dedicate this dissertation to graduate students everywhere.

Contents

List of Figures

List of Tables

Acknowledgments

Too bad nobody helped me.

Chapter 1

Introduction

Abstract.

1.1 Introduction

1.2 Symmetric and antisymmetric critical current noise

[The following needs a lot of work! The only point is that asymmetric variations can't be much larger than symmetric variations.]

[Newer version (outline form):]

Suppose that a single junction has a noise spectrum S_{I_0}. Then symmetric critical current variations of the SQUID will have noise spectrum $S_{I_c,\mathrm{sym}} = 2S_{I_0}$. There's a factor of 2 because the noise between junctions is uncorrelated. While asymmetric critical current variations do not directly change the critical current, they can indirectly change the critical current by inducing a flux. Asymmetric variations induce a circulating current that can, through the self-inductance of the SQUID, induce a flux. [What is the magnitude of the circulating current?? Isn't it just S_{I_0}?]

$$S_{I_c,\mathrm{asym}} = S_{I_0} L^2 \left(\frac{\partial I_c}{\partial \Phi}\right)^2 \tag{1.1}$$

Next, because $|\partial I_c/\partial\Phi|_{\max} \sim I_c/\Phi_0$ and $\beta_L = LI_c/\Phi_0$,

$$S_{I_c,\mathrm{asym,max}} \sim S_{I_0}(LI_c/\Phi_0)^2 = S_{I_0}\beta_L^2 \lesssim S_{I_0}. \tag{1.2}$$

Therefore, critical current noise due to asymmetric variations will never be much larger than that due to symmetric variations.

[Old version:]

The symmetric component of critical current noise $S_{I_c,\mathrm{sym}}$ is independent of flux bias. However, because of the antisymmetric component $S_{I_c,\mathrm{asym}}$, which couples to the SQUID

as a flux and therefore adds noise proportional the the flux sensitivity of the SQUID, the magnitude of the noise can vary with flux bias:

$$\frac{\partial I_{\text{loop}}}{\partial I_{c,\text{asym}}} = L^2 \left(\frac{\partial I_{\text{loop}}}{\partial \Phi_m} \right)^2, \tag{1.3}$$

where L is the self-inductance of the SQUID. Because the maximum $\partial I_{\text{loop}}/\partial_m$ varies roughly as I_c/Φ_0 for our devices, which have $\beta_L \equiv LI_c/\Phi_0 \lesssim 0.5$, Eq. (1.4) can be approximated as

$$\left(\frac{\partial I_{\text{loop}}}{\partial I_{c,\text{asym}}} \right)_{\text{max}} \approx \left(\frac{\beta_L \Phi_0}{I_c} \right)^2 \left(\frac{I_c}{\Phi_0} \right)^2 \approx \beta_L^2. \tag{1.4}$$

Because critical current variations within the junctions are independent, $S_{I_c,\text{sym}} = S_{I_c,\text{asym}}$. Therefore, we see that the maximum noise contribution due to asymmetric critical current variations is of the same order of magnitude as, or much lower than, that of symmetric variations. Furthermore, because the magnitude of $S_{I_c,\text{asym}}$ varies with SQUID inductance, which is often difficult to measure, it is difficult to know accurately.

Acknowledgments

Too bad nobody helped me with the introduction either.

Chapter 2

Dephasing in qubits due to flux noise

[This chapter will essentially be the PRB that we published.]

Chapter 3

Numerical calculations of the mean square flux noise

Chapter 4

Experimental measurement system and procedures

4.1 Overview

Thus far we have considered flux noise in SQUIDs and qubits in a theoretical context. However, the bulk of our work is concerned with the experimental characterization of flux noise in SQUIDs. The success of this endeavor relies on a robust experimental measurement system that satisfies a number of stringent requirements. First and foremost, because we seek to accurately measure the intrinsic noise in SQUIDs, which are themselves ultra-low-noise devices, every care must be taken to insure that the measurement system produces as little noise as possible. In this same thread, $1/f$-noise measurements at low frequencies are necessarily slow measurements, which entails that the system must be ultra-stable over time scales on the order of hours. As noise originating from myriad sources—electronic and mechanical as well as temperature and magnetic field fluctuations, for example—can couple into the measurement, the design considerations are considerable.

We also seek to characterize the flux noise as a function of device temperature, which means that we need a refrigeration apparatus that can hold a stable temperature from approximately 0.1 K up to 4 K. Standard dilution refrigerators are quite capable of reaching such temperatures, but we shall see that care is needed to achieve the required stabilities well in excess of 1 part in 10^4.

For a number of reasons, it is advantageous for the system to have the ability to cool multiple SQUIDs in a single cool-down and to measure each one individually. On one hand, the length of the cool-down and warm-up procedures of our dilution refrigerator means that considerable time is saved over cooling each SQUID individually. On another hand, cooling several SQUIDs simultaneously eliminates many potential confounding factors—trapped magnetic fields, for example—that could conceivably cause differences between measurements from different cool-downs.

In this Chapter we review the experimental design and implementation as well as the validation, calibration, and measurement procedure. The main components of the system

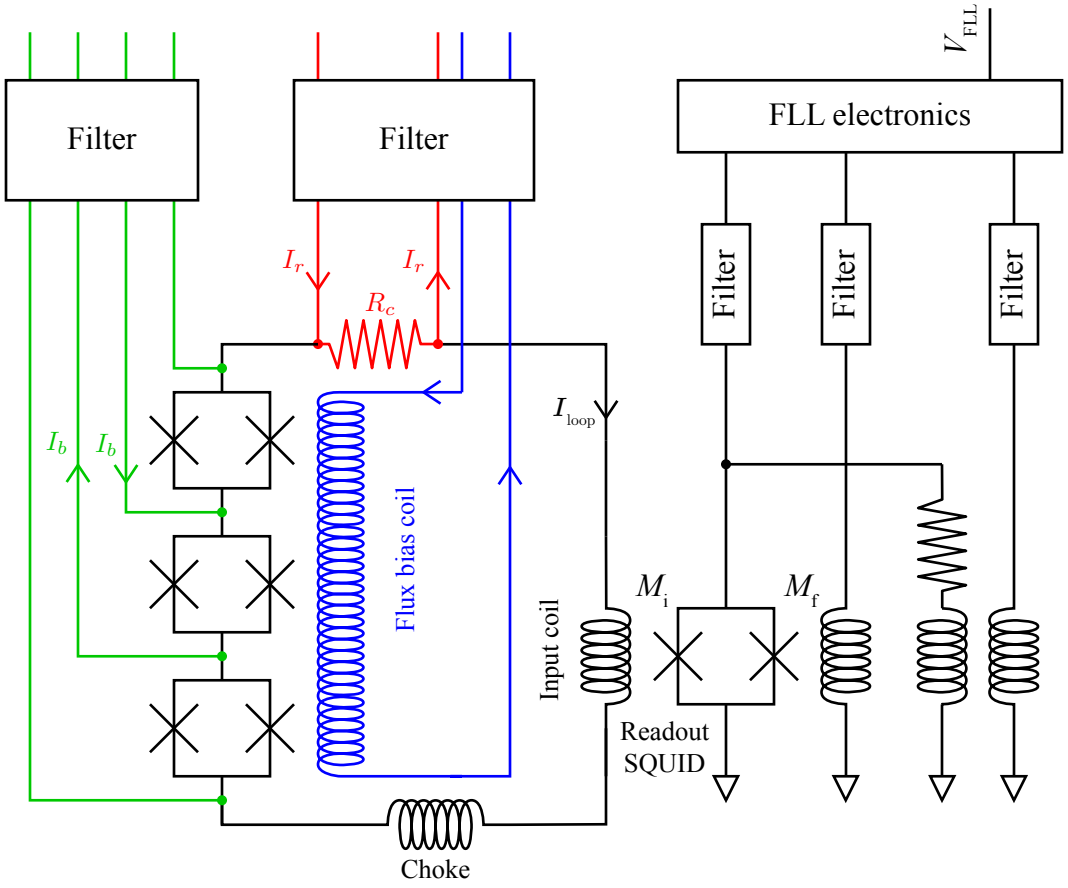

Figure 4.1: Configuration of measurement system to measure flux noise in three SQUIDs. The bias current I_b shown enables the measurement of the middle SQUID. The static voltage across the SQUID is canceled by the current I_r applied to the compensating resistor R_c. [@@@ transformer ratios]

are the [@@@ probably put the sections here], which we now discuss in detail.

4.2 Measurement overview

The principle behind our measurement technique is that a SQUID biased into the normal state generates fluctuations based on changes in its critical current and the flux through its loop. Naturally, these fluctuations are quite small and cannot be read directly using even the best room-temperature amplifier. Therefore, we use a second SQUID, operated in a standard flux-locked loop (FLL) configuration, to detect the fluctuations. The fluctuations of the measured SQUID are monitored for long periods of time, converted to spectral densities, and subsequently analyzed.

The basis of our system is the circuit schematic illustrated in Fig. 4.1, where we have modified the design used by Wellstood [1] in order to accommodate multiple measured SQUIDs. In the circuit, several SQUIDs are connected in series with a small compensating resistor R_c, the input coil to the readout SQUID, and a choke inductor, which prevents high-frequency cross-talk between SQUIDs. Appropriate wiring to the circuit allows us to inject currents across the compensating resistor and each of the SQUIDs. To make a measurement, we begin by injecting a current I_b through a particular SQUID and increasing it until the SQUID enters the normal state with voltage V_{SQUID}. At this point, most of the current bias passes through the measured SQUID, but a small amount V_{SQUID}/R_c is shunted through the compensating resistor. If I_b is increased further, a fraction $R_c/(R_d + R_c)$ of the current passes through the compensating resistor, where R_d is the dynamic resistance of the measured SQUID. For reasons we discuss later, $R_c \ll R_d$ by design. If large enough, the shunted current that flows around the big loop can drive the other SQUIDs normal, where they begin to add their own intrinsic noise. To prevent this, a current I_r is passed through the compensating resistor until $V_{\mathrm{SQUID}} = I_r R_c$ and no net current flows around the loop, ensuring that the SQUIDs not under measurement remain superconducting and contribute no noise.

At this point, a variation in the critical current of the SQUID will redistribute the bias currents to the circuit. For instance, if the critical current suddenly drops, a fraction of I_b will be diverted around the big loop, through R_c and the input coil, thereby introducing a flux offset in the readout SQUID. The FLL, which is operated above 100 kHz, rapidly cancels this offset by increasing the current to a feedback coil (Fig. 4.1) until the flux offset is canceled. A voltage V_{FLL} proportional to the feedback current and, correspondingly, the current circulating the loop is read at the output of the FLL. For small variations in the measured SQUID, the response is linear so that V_{FLL} is also proportional to both the critical current of the SQUID. We now discuss the conversion factors as well as our choice of circuit and device parameters, chosen to optimize the sensitivity to the fluctuations.

Operated in this configuration, any single measurement is insufficient to discern the origin of the fluctuations that we measure. The noise we measure could originate from intrinsic critical current noise within the junctions; flux noise in the SQUID, which, in turn, modulates the critical current of the SQUID; or noise in the measurement or bias circuitry. Therefore, to verify our SQUID noise measurements, we must first verify that the noise of our bias and readout circuitry is negligible. Next, in order to distinguish between critical current and flux noise, we utilize the property of the SQUID whereby its sensitivity to flux ($\partial I_c/\partial \Phi$) varies as a function of its flux bias [@@@ ref in Chap 1]. By varying the flux bias and corresponding sensitivity of the SQUID, we can verify that the noise from the various spectra scales as an effective flux.

4.2.1 Optimal circuit and device parameters

In general, we choose parameters to maximize the change in V_{FLL} for a given change in critical current or flux in the measured SQUID. First, we discuss the value of the compensating resistor. In Fig. 4.2(a) we show a simplified schematic of the typical biasing of a

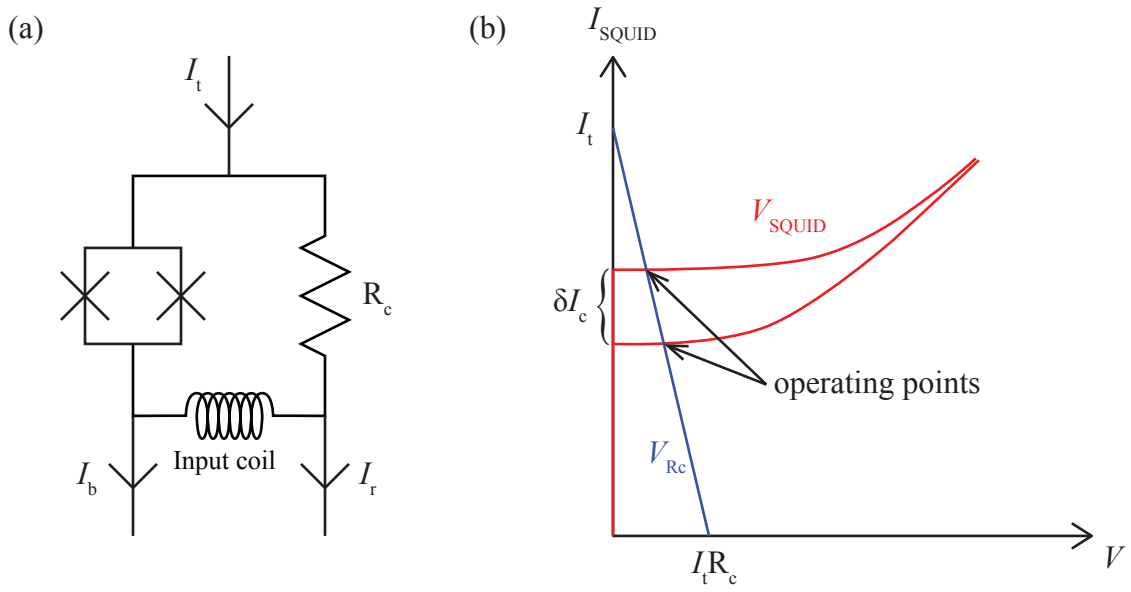

Figure 4.2: Bias and operating points of measured SQUID. (a) Simplified schematic of the typical biasing of a measured SQUID. (b) Current-voltage characteristics of a SQUID (red) for a small change in critical current. The load line for R_c (blue) is calculated as follows. For zero current flowing through R_c, $V_{R_c} = 0$ and the current through the SQUID, I_{SQUID}, is maximum: $I_{\mathrm{SQUID}} = I_t$. For $I_{\mathrm{SQUID}} = 0$, the total current flows through R_c and $V_{R_c} = I_t R_c$. The equilibrium solution occurs when $V_{\mathrm{SQUID}} = V_{R_c}$, which is the intersection of the two curves. Therefore, δI_c causes the operating points to change little in voltage, but maximally in current.

SQUID, omitting the superconducting SQUIDs; here, $I_t = I_r + I_b$ is the total current applied to the circuit. Ultimately, we seek to maximize the change in current through the input coil for a given change in SQUID critical current, I_c. In this familiar circuit, we recognize that if $R_c \gg R_d$, the SQUID is effectively current biased. That is, if the critical current of the SQUID decreases slightly, V_{SQUID} will increase by δV and the current through R_c will increase by only $\delta V/R_c$, which, by construct, is very small. However, if $R_c \ll R_d$, the SQUID is effectively voltage biased. We show this situation in Fig. 4.2(b), using the concept of load lines because the SQUID is a nonlinear circuit element. In this scenario, a decrease ΔI_c in the I_c of the SQUID corresponds to a maximum increase in increase of current through R_c and, correspondingly, the input coil of the readout SQUID ΔI_{loop},

$$\Delta I_{\mathrm{loop}} = \frac{1}{1 + R_c/R_d} \Delta I_c. \tag{4.1}$$

For typical values of $R_d \sim 10\ \Omega$, R_c should be on the order of 1 Ω. From Eq. (4.1), we see that values of R_c much less than $R_d/10$ do not offer much additional signal and can, in fact, degrade the performance of the system if R_c is too low. We also see that for $R_c \ll R_d$, $\Delta I_{\mathrm{loop}} \approx \Delta I_c$ and throughout this thesis we will often use ΔI_{loop} and ΔI_c interchangeably.

With a small value of R_c, we ensure that fluctuations in the readout SQUID generate maximum current fluctuations through the input coil of the readout SQUID. In turn, we maximize the flux coupled into the readout SQUID by using the largest feasible mutual inductance for the input coil M_i. In general, $M_i \sim 10$ nH, or $M_i^{-1} \sim 0.1\ \mu\mathrm{A}/\Phi_0$. Conversely, we aim to make the mutual inductance of the feedback coil M_f small (~ 0.5 nH) so that the feedback current is relatively large. Finally, the feedback resistor R_{feedback}, which sets the conversion factor between the feedback current and V_{FLL}, is chosen to be large ($\gtrsim 100\ \mathrm{k}\Omega$). Thus, V_{FLL} is related to I_{loop} via

$$V_{\mathrm{FLL}} = R_{\mathrm{feedback}} \left(\frac{M_i}{M_f} \right) I_{\mathrm{loop}}, \tag{4.2}$$

and the FLL has a transconductance on the order of 10^6 V/A.

It is also possible to optimize the junction parameters of the SQUIDs. By varying the value of the shunt resistance R and critical current of the junctions, we can modify the level of white noise and flux sensitivity, respectively. At high enough frequencies—typically, above 10 to 100 Hz when the SQUID is biased at maximum flux sensitivity—the white noise generated by the shunt resistors dominates both the flux and critical current noise of the SQUID. As a current, the white noise magnitude scales as R^{-1} [2] [@@@ cover in Chap 1], which indicates that we can reduce the white noise level by increasing R. Because $\partial I_c/\partial \Phi$ is roughly proportional to I_c [@@@ cover in Chap 1], we can also increase the sensitivity of our measurement to flux in the measured SQUID. These two criteria suggest that one should increase R and I_c as much as possible in order to maximize the relative current variations due to flux noise. However, our measurements require that the SQUIDs operate non-hysteretically, that is, $\beta_c = 2\pi I_0 R^2 C/\Phi_0 < 1$ [3, 4], so that R and I_0 cannot both be

increased without bound. Here, $I_0 = I_c/2$ and C are the average junction critical current and capacitance, respectively. For fixed critical current density j_c and constant capacitance per unit area C/A, I_0 is typically varied by changing the junction area A so that $I_c R^2 C \propto A^2 R^2$. Assuming that one designs a SQUID for fixed $\beta_c < 1$, this constraint also implies a fixed product $I_c R$. Because the white noise decreases only as R^{-1} but the flux sensitivity increases as $(\partial I_c/\partial \Phi)^2 \propto I_c^2$, we see that it is most advantageous to increase I_c as much as possible, even at the cost of decreasing R.

4.3 Implementation

We now discuss the specifics of how we implement the measurement system, which is shown schematically in Fig. 4.3. The SQUIDs to be measured, which are typically fabricated onto a single chip, are first mounted and wire-bonded onto a circuit board in one of the chambers of a copper sample box (Fig. 4.4). Flux bias is provided via either an on-chip coil or a coil mounted in the circuit board, directly below the chip. The compensating resistor, which is simply a short segment of resistance wire, is also mounted to the circuit board. The readout SQUID is located in another chamber on the opposite side of the box in order to prevent cross-talk between SQUIDs. Intermediate chambers contain the choke inductor and a cold transformer on the voltage line of the readout SQUID, which is used both to step up the voltage and to impedance match to the room-temperature amplifier. Once the sample is mounted into the box, a Cu lipped lid is attached. For magnetic shielding, the inner surfaces of both the box and lid are electroplated with approximately 200 μm of Pb.

The sample box is then mounted onto the cold finger of an Oxford DR200 dilution refrigerator. In addition to the Pb plating of the sample box, further attenuation and shielding of external magnetic fields are provided by two concentric cans of Pb and Cryoperm. Electrical signals are carried via three 4-conductor Reichenbach cables for the various biasing of the measured SQUIDs and three SMA coaxial cables for the current bias, voltage readout, and flux feedback current of the readout SQUID. All lines are rf-filtered using standard copper powder filters (CPFs) and low-pass filtered using discrete filters. Bias currents are provided via lithium-ion battery-powered boxes using one of two circuit designs, shown in Fig. 4.5. The current biases for I_b and I_r typically need to source only tens of microamps and use the "passive" design [Fig. 4.5(a)]. The current bias for the flux bias of the measured SQUIDs, however, can require in excess of 10 mA, so we use an "active" source [Fig. 4.5(a)]. Both designs rely on the extremely flat discharge voltage of Li-ion batteries, which allows us to use them as simple, yet stable, voltage references. For the readout and control electronics of the FLL, we have used two different commercial packages available from Easy SQUID and STAR Cryoelectronics, respectively. Both packages come with amplification units, which we attach directly atop the fridge. For additional isolation and electric shielding, the fridge and the electronics mentioned thus far are located within a shielded room, consisting of an electrically continuous copper sheet (Fig. 4.3).

The FLL preamplification box interfaces with the control electronics, external to the

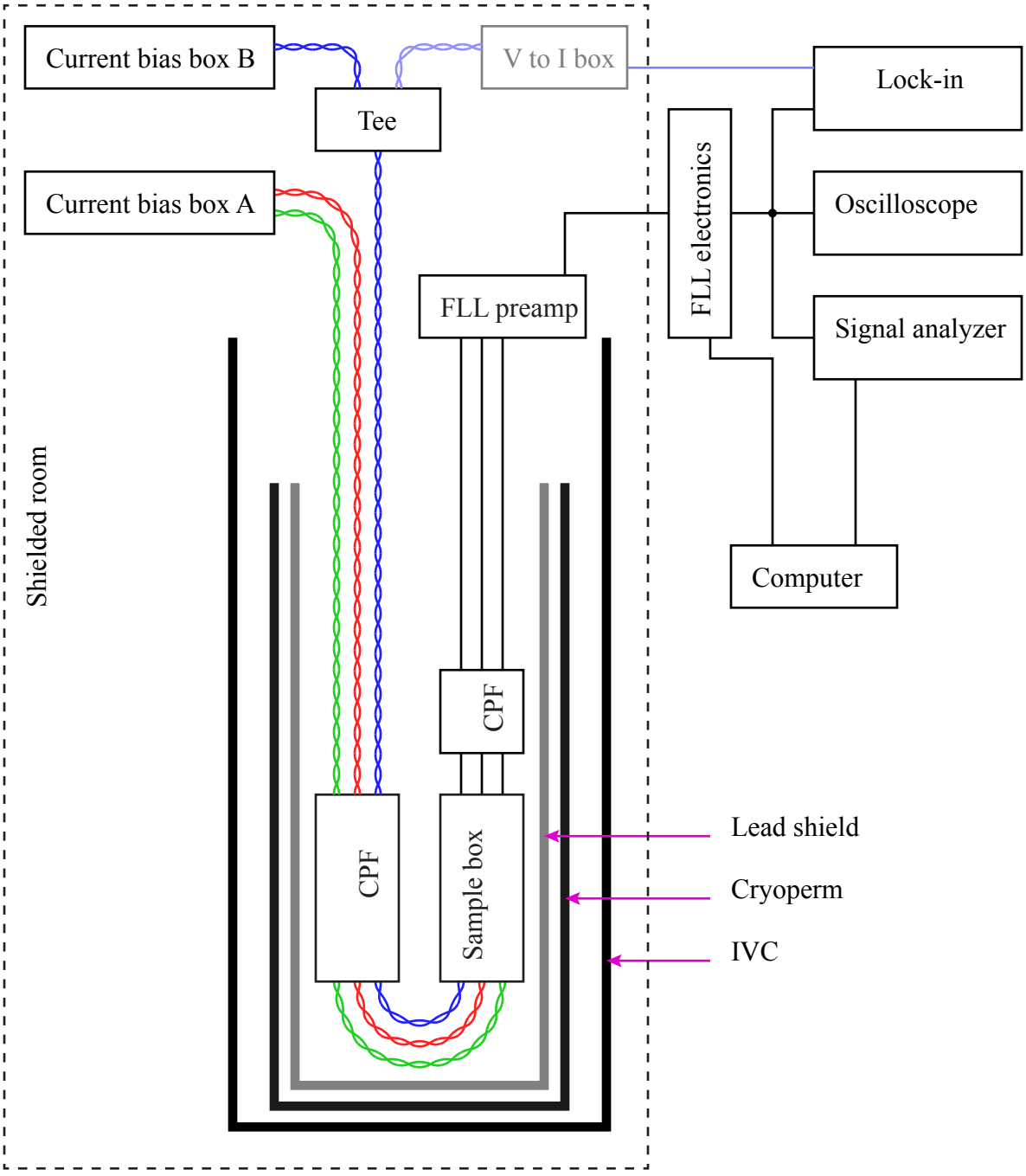

Figure 4.3: Schematic of measurement system. The sample is mounted to the cold finger of a dilution refrigerator and is surrounded by a combination shield of Pb and Cryoperm for magnetic shielding. All lines are low-pass filtered using copper powder filters (CPF) and discrete filters. The typical configuration of bias boxes and readout equipment is shown. The shaded portion is connected only when measuring $\partial I/\partial\Phi$, not when acquiring noise data. [@@@ This fig probably runs over the bottom margin! @@@ Add discrete filters]

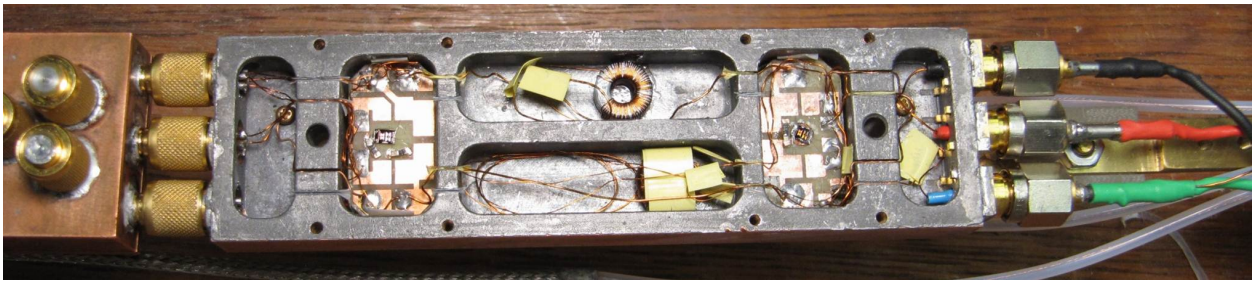

Figure 4.4: Photo of sample box. Six chambers separate the various portions of the measurement circuit. The circuit board holding the measured SQUIDs is on the left. On the right is the board holding the readout SQUID. The chambers in the middle hold the choke inductor and cold transformer, wound around molypermalloy powder (MPP) cores, which work well at cryogenic temperatures.

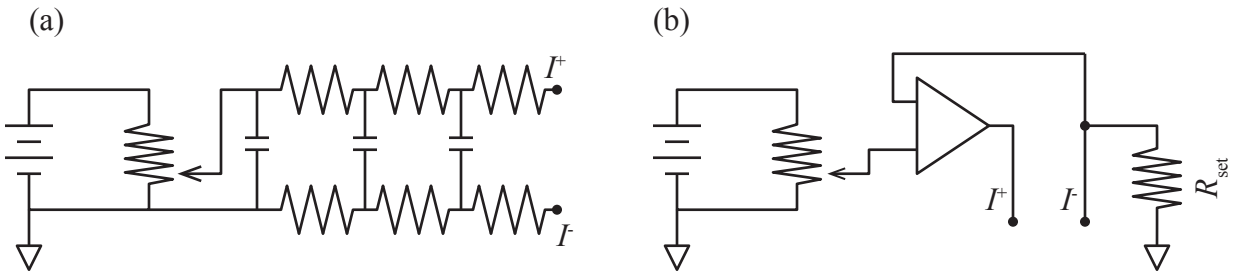

Figure 4.5: Circuit schematics of current supply boxes. (a) "Passive" circuit design, type A. Li-ion battery sources a current controlled by a 10-turn potentiometer. This design is useful for sourcing $\lesssim 100\ \mu$A. (b) "Active" circuit design, type B. The Li-ion battery and 10-turn potentiometer provide a stable voltage source input to the op-amp (ISL28134). R_{set} sets the current output range, which, for this op-amp, is approximately 60 μA. Since the op-amp sources the current, the discharge on the Li-ion batter is minimal.

shielded room, via a filtered DB9 cable. The FLL control electronics in turn output V_{FLL} and also connect to a computer, which provides control over the FLL parameters. The output V_{FLL} is passed to a oscilloscope, which is used during the biasing procedure, and to an Agilent 35670A signal analyzer. It is also passed to a lock-in amplifier, which is used to measure $\partial I/\partial\Phi$, which is described in Section 4.5.

Data are acquired using the signal analyzer and sent to a computer for analysis and storage. Under normal operation, the signal analyzer acquires data and computes the spectral density, which is stored in a buffer that the computer can access. However, we have found that it is much more advantageous to use the signal analyzer to capture the raw time series of V_{FLL}. A single time capture allows us to compute multiple FFT's with differing numbers of averages to form a single, stitched spectrum. [Appendix on how this is done?] In a typical measurement, the sampling rate and length of time capture, which defines the buffer size, are programmed into the signal analyzer via the computer interface and a custom LabVIEW program (Signal Analyzer Controls in Fig. 4.6). The signal analyzer then fills the buffer and uploads the time series to the LabVIEW program, where we can save it to disk, together with a header file with details of the measurement, and compute the spectral density. For more advanced plotting and analysis functions, we use a suite of Matlab programs that we have written for this purpose.

[@@@ anything else?]

4.4 Calibration and validation

To validate the system, we must first measure certain parameters in order to calibrate conversion factors and then verify that the readout and bias electronics are sufficiently low-noise. First, we seek to calibrate the output of the FLL; that is, we want to know $\partial I_{\mathrm{loop}}/\partial V_{\mathrm{FLL}}$. From Eq. (4.2), this means we need to measure M_i, M_f, and R_{feedback}. There is a trick, however, that allows a direct calibration of $\partial V_{\mathrm{FLL}}/\partial\Phi_a$, where Φ_a is the flux in the readout SQUID. Then,

$$\frac{\partial I_{\mathrm{loop}}}{\partial V_{\mathrm{FLL}}} = \left(\frac{\partial I_{\mathrm{loop}}}{\partial \Phi_a}\right)\left(\frac{\partial \Phi_a}{\partial V_{\mathrm{FLL}}}\right) = M_i^{-1}\left(\frac{\partial V_{\mathrm{FLL}}}{\partial \Phi_a}\right)^{-1}. \tag{4.3}$$

To measure $\partial V_{\mathrm{FLL}}/\partial\Phi_a$, we begin by locking the FLL with zero current in the big loop and we record the V_{FLL}. Next, we unlock the FLL, inject a current into the input coil corresponding to approximately one flux quantum, and lock the loop. We can do this even with the SQUIDs bonded into the loop by injecting a current I_r across the compensating resistor. Since the SQUIDs are superconducting, the current will flow through the lowest resistance path; that is, all the current will flow through the SQUIDs and input coil. With the loop locked, we now reduce the bias current back to zero and again record V_{FLL}. The difference in recorded voltages ΔV_{FLL} corresponds to one Φ_0 in the readout SQUID, $\partial V_{\mathrm{FLL}}/\partial\Phi_a = \Delta V_{\mathrm{FLL}}/\Phi_0$, which is about 0.5 V/$\Phi_0$ for our system. This method is described in detail in Sec. 2.10a of Ref. [1]. The mutual inductance of the input coil M_i can be readily measured by injecting

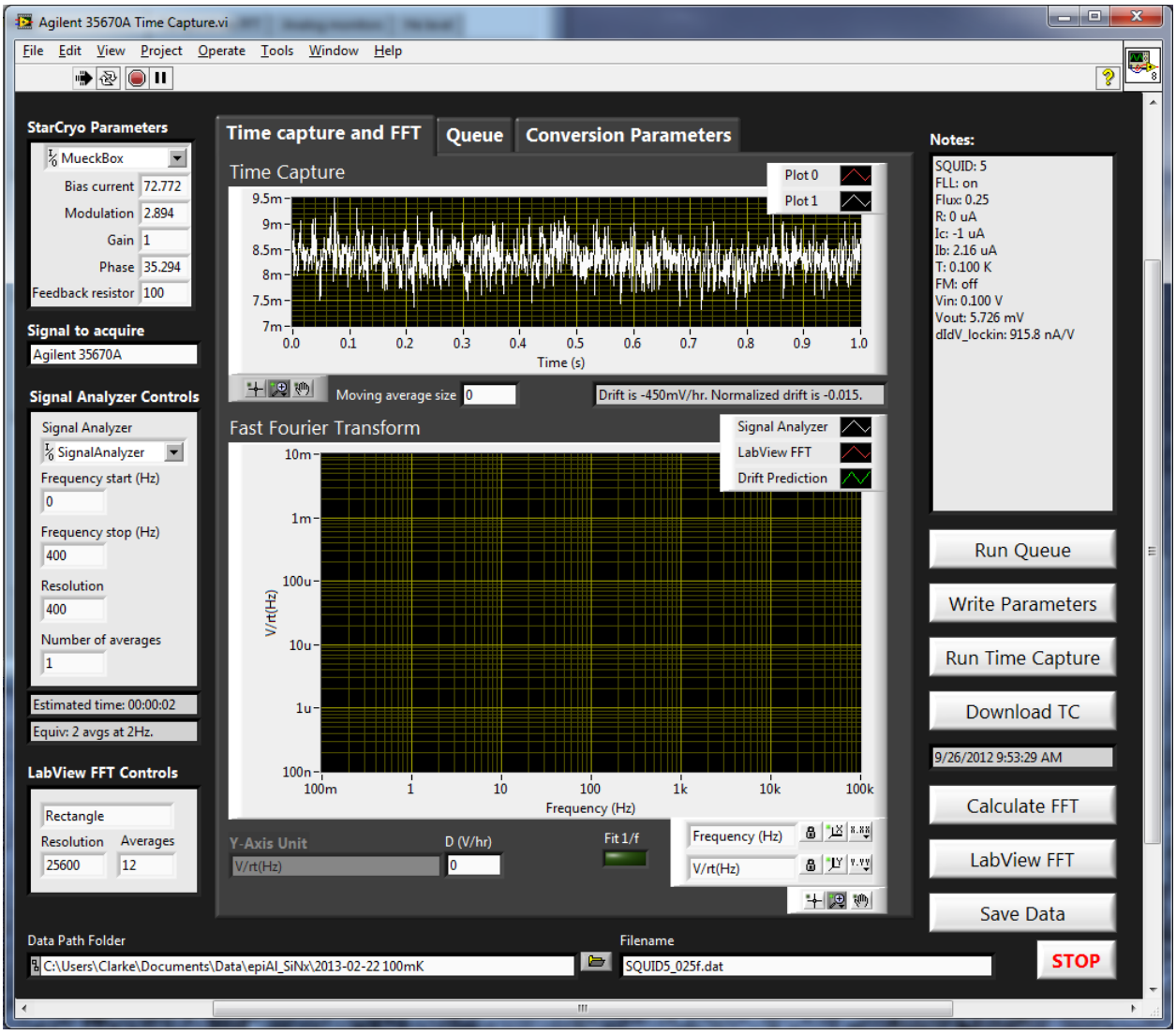

Figure 4.6: Screenshot of LabVIEW time capture acquisition program. For a typical measurement, 'Signal Analyzer Controls' set the sampling frequency and buffer size of the signal analyzer. 'Run Time Capture' instructs the signal analyzer to start filling the buffer. Once the time capture finishes and is downloaded, we can compute the FFT in LabVIEW with parameters set in 'LabVIEW FFT Controls'. A 'Notes' section allows the user to specify details of the measurement; these notes, along with the parameters of 'Signal Analyzer Controls' are saved to the specified file and path. Several different time captures can be queued to run sequentially. [@@@ Need to take better capture and add FFT.]

a known bias current into the circuit—again, across the compensating resistor if SQUIDs are in the circuit—and measuring the response in V_{FLL}. For $M_i \approx 10$ nH as in our system, $\partial I_{\mathrm{loop}}/\partial V_{\mathrm{FLL}} \approx 0.4$ μA/V.

Next, we must calibrate V_{FLL} to changes in the measured SQUID. Changes in I_c are related to V_{FLL} via

$$\frac{\partial I_c}{\partial V_{\mathrm{FLL}}} = \left(\frac{\partial I_c}{\partial I_{\mathrm{loop}}}\right)\left(\frac{\partial I_{\mathrm{loop}}}{\partial V_{\mathrm{FLL}}}\right) \approx \frac{\partial I_{\mathrm{loop}}}{\partial V_{\mathrm{FLL}}} \tag{4.4}$$

by Eq. (4.1) for $R_c \ll R_d$. For our applications, Eq. (4.4) is sufficiently accurate—10% for $R_c = R_d/10$—as we are not focused on highly accurate measurements of critical current noise.

To scale V_{FLL} to an equivalent flux noise, we seek to measure the change ΔV_{FLL} in response to a known applied flux in the measured SQUID $\Delta\Phi_m$. In order to do so, we must first measure the mutual inductance M_m between the flux bias coil (which is either fabricated on-chip or mounted in the circuit board to which the chip is mounted) and the measured SQUID. We readily accomplish this by injecting a known current I_Φ into the coil and monitoring the response of the SQUID, which is periodic in flux. For example, the difference in flux, achieved by a difference in current ΔI_Φ in the coil, that separates maxima in SQUID critical current is 1 Φ_0. Therefore, the mutual inductance is simply $M_m = \Phi_0/\Delta I_\Phi$. In principle, only one period is sufficient for this measurement, but we typically measure over five or more and perform a linear regression for better accuracy. In addition, we have found that measuring the flux bias corresponding to a minimum SQUID critical current, rather than a maximum, is more precise because the I_c–Φ characteristics are much sharper at $(n+\frac{1}{2})\Phi_0$ than at $n\Phi_0$. Finally, to measure $\partial V_{\mathrm{FLL}}/\partial\Phi_m$ we inject a known current, converted to a flux in the measured SQUID via M_m, and measure the response in V_{FLL}. This calibration, which must be performed before each flux noise measurement, is described in greater detail in the next Section.

After establishing the relevant conversion factors, we want to characterize the noise of the measurement system. With the measured SQUIDs in the superconducting state, the major sources of noise are (i) the amplification and readout electronics of the FLL, (ii) the intrinsic critical current and flux noise of the readout SQUID, and (iii) the Nyquist noise of the compensating resistor [5]. While it is possible to measure the noise from (i) and (ii) independently, the characterization process is complicated, lengthy, and involves several cooldowns to 4 K. A much simpler method exists that puts an upper bound on the combined noise of (i) and (ii). With accurate knowledge of the compensating resistance R_c and temperature T, we can calculate the Nyquist current noise spectral density as $S_{I,R_c} = 4k_BT/R_c$. By comparing the measured to predicted noise, we can estimate the noise added by the readout. In addition, we can confirm the calibration of the system. We find that our electronics add approximately 3 $(\mathrm{pA})^2/\mathrm{Hz}$ of white noise, which is negligible compared to S_{I,R_c} for $T \gtrsim 0.3$ K and $R_c \approx 0.5$ Ω. Above this temperature, agreement between measurement and prediction is better than 10%. This measurement also yields the $1/f$ noise of (i) and (ii); (iii) contributes no $1/f$ noise. We found that the Easy SQUID readout system

exhibited significantly more $1/f$ noise than the Cryoelectronics, which was a problem when measuring low-noise SQUIDs.

Finally, we remark that [temperature noise, explained in detail in Appendix?]

4.5 Measurement procedure

[The following section probably needs a bit more detail.]

The SQUID is variably sensitive to small changes in flux depending on its flux bias, ranging from zero sensitivity when biased at $n\Phi_0$ to maximum sensitivity at nominally $(n \pm \frac{1}{4})\Phi_0$. To measure flux noise, clearly we must bias the SQUID at a point where it is sensitive to changes in flux. However, as discussed in Chapter 1, the total noise generated by the SQUID includes both critical current and flux noise. Furthermore, the magnitude of the contribution of asymmetric critical current variations varies as the flux sensitivity. Therefore, if the critical current noise is significant compared to the flux noise, its contribution is very difficult to subtract accurately from the total noise. If the critical current noise is much smaller than the flux noise, however, we can safely neglect its contribution. Therefore, we first characterize the critical current noise of the SQUID to ensure that it is negligible and then we measure at maximum flux sensitivity.

To measure the critical current noise of a SQUID we first bias it into the voltage state—typically $V_{\mathrm{SQUID}} \sim 5\ \mu$V—and null the induced loop current I_{loop} with an appropriate current through the compensating resistor. At this point, we vary the flux bias Φ_m—adjusting the current bias I_b as the critical current changes—to the point where I_c is maximum and $\partial I_c/\partial\Phi_m = 0$, which corresponds to a flux bias of $n\Phi_0$. In this situation, a symmetric variation in the critical currents of the junctions will cause I_c to vary, which, in turn, induces a current I_{loop} into the input coil of the readout SQUID as in Eq. (4.1). We acquire a time capture of V_{FLL}, sampled at approximately 1 kHz, for between 15 minutes to 1 hour, which is sufficiently long to characterize the noise at low frequencies (down to approximately 10^{-1} Hz to 10^{-2} Hz). From the time capture, we compute the spectral density, which we can scale to an equivalent current in the loop via Eq. (4.3). At high frequencies, the spectrum is flat due to the white noise generated by the resistive shunts of the junctions. If the magnitude is large enough, the $1/f$ noise from symmetric critical current fluctuations will cause the observed spectral density to increase at low frequencies.

Once the critical current noise is characterized, we next seek to bias the SQUID at the point of maximum sensitivity to flux in order to measure its flux noise. In other words, we vary Φ_m until $\partial I_{\mathrm{loop}}/\partial\Phi_m$ is maximized. To measure $\partial I_{\mathrm{loop}}/\partial\Phi_m$, we first use the internal oscillator of a Stanford Research Systems SR830 lock-in amplifier and a custom voltage-to-current box to generate an oscillating current of known magnitude. As shown in Fig. 4.3, the oscillating current is summed with the static flux bias current and injected into the flux bias coil of the measured SQUID. Using the measured value of M_m, we calculate the rms magnitude of oscillating flux $\Phi_{m,\mathrm{osc}}$ applied to the measured SQUID. The oscillating flux causes I_c and, correspondingly, V_{FLL} to modulate. We use the lock-in to demodulate V_{FLL}

Figure 4.7: Noise spectra versus bias.

Figure 4.8: Proper scaling of flux noise. Noise spectra acquired at different values of $\partial I_{\rm loop}/\partial\Phi_m$.

and compute the rms magnitude of the voltage oscillations $V_{\rm FLL,osc}$, from which we readily calculate

$$\frac{\partial I_{\rm loop}}{\partial \Phi_m} = \frac{V_{\rm FLL,osc}}{\Phi_{m,\rm osc}} \left(\frac{\partial I_{\rm loop}}{\partial V_{\rm FLL}} \right). \tag{4.5}$$

To ensure that the response is linear, it is important that $\Phi_{m,\rm osc} \ll \Phi_0$; in our measurements, $\Phi_{m,\rm osc}/\Phi_0$ was typically between 10^{-2} and 10^{-3}. Depending on the value of β_L, the flux bias corresponding to maximum $\partial I_{\rm loop}/\partial\Phi_m$ can vary from approximately $(n \pm \frac{1}{4})\Phi_0$ for SQUIDs with $\beta_L \approx 1$ to very near $(n \pm \frac{1}{2})\Phi_0$ for SQUIDs with $\beta_L \ll 1$ [6]. In spite of this detail, for brevity we will often refer to $\Phi_m = \frac{1}{4}\Phi_0$ as the bias corresponding to the maximum sensitivity.

With $\partial I_{\rm loop}/\partial\Phi_m$ maximized, we voltage bias the SQUID and null $I_{\rm loop}$ in the manner previously described, acquire a 1 hr time capture, and compute the spectral density. At this flux bias, I_c is maximally sensitive to both asymmetric critical current and flux noise. By comparing this spectrum to that acquired at $n\Phi_0$, we can readily determine the noise added by these two sources. We recall from our previous discussion in Sec. 1.2 that I_c variations due to asymmetric critical current variations are generally smaller than I_c variations due to symmetric critical current variations: $S_{I_c,\rm asym} \lesssim S_{I_c,\rm sym}$. Therefore, a large difference in noise between the two spectra must be due to the flux noise. [@@@ Talk about Fig. 4.7]

As a further verification, we can verify that the observed noise increase scales as an equivalent flux. To do this, we reduce $\partial I_{\rm loop}/\partial\Phi_m$ to, say, half its maximum and again acquire data. If the observed noise is indeed due to flux variations, its magnitude referenced as a current in the input coil should scale as $(\partial I_{\rm loop}/\partial\Phi_m)^2$; that is, the spectral density at a particular frequency should be reduced by a factor of four compared to the spectrum acquired at $|\partial I_{\rm loop}/\partial\Phi_m|_{\rm max}$. Of course, the white noise from the shunts, which dominates at high enough frequency, does not scale as a flux, so the "knee" between white current noise and $1/f$ flux noise will decrease in frequency, a fact that highlights the importance of acquiring data at maximum $\partial I_{\rm loop}/\partial\Phi_m$. [@@@ Reference Fig. 4.8]

4.6 Fits?

After acquiring...
Appendix A

4.6.1 Lorentzian fits?

4.7 Low-frequency critical current noise

[Make this an appendix instead?]

Appendix A

Calculating a stitched spectrum from time series

Many existing programs and scripts exist that compute the fast Fourier transform (FFT) and corresponding spectral density of an input time series. However, for a number of reasons we have found it advantageous to compute several FFT's from the time capture and to "stitch" them together to represent the spectrum. In this Appendix, we review our algorithm to compute the FFT's and to stitch them into a single spectrum.

Given an input time series, sampled at a frequency $1/\Delta t$ and consisting of N points of amplitude y_j ($j \in \{1, 2, 3, \ldots\}$), the FFT is defined as

$$Y_k = \sum_{j=1}^{N} y_j \omega_N^{(j-1)(k-1)}, \tag{A.1}$$

where $\omega_N = \exp[-2\pi i/N]$ is an N^{th} root of unity. In general, the FFT algorithm works best when N is a power of 2; if it is not, y_j is usually padded with zeros until its length is a power of 2. Because $y_j \in \mathbb{R}$, Y_k is symmetric ($Y_k = Y^*_{N-k+2}$ for $k \geq 2$) and the power spectral density S_k can be written as

$$S_k = \begin{cases} \frac{\Delta t}{N}|Y_1|^2 & \text{if } k = 1 \\ 2\frac{\Delta t}{N}|Y_k|^2 & \text{if } k \in \{2, 3, 4, \ldots N/2 + 1\} \end{cases}, \tag{A.2}$$

which is defined at frequencies $f_k = (k-1)/N\Delta t$, where $k \in \{1, 2, 3, \ldots N/2 + 1\}$.

One can compute a single FFT of the entire time capture ($N = N_{\text{tc}}$). However, this technique leads to a spectrum that appears extremely noisy; that is, the difference between the spectral density at adjacent frequencies is of the order of the spectral density itself, regardless of the length of the time capture. This property can be understood as follows. At any particular frequency, S_k of a random time series follows a Chi-squared distribution with two degrees of freedom ($S_k \sim \chi^2_2$). A property of the χ^2_2 distribution is that the variance σ^2 is equal to its mean μ squared. Therefore, $\sigma^2(S_k) = \mu^2(S_k)$ so that the spread of

spectral densities is relatively large and the spectrum appears noisy. A longer time capture increases $N_{\rm tc}$, which in turn increases the frequency resolution—the width of the frequency bins $df = 1/N\Delta t = 1/N_{\rm tc}\Delta t$—but do not decrease $\sigma^2(S_k)$.

To reduce the apparent noise in the spectrum, it is typical to introduce some form of averaging. A popular method is to split the time capture into $N_{\rm avg}$ equivalent-length segments, computing the FFT for each segment and averaging the spectral densities to form a single averaged spectrum. In other words, $S_k = (1/N_{\rm avg}) \sum S_{k,n}$, where S_k is now an averaged spectral density and $S_{k,n}$ is the spectral density at f_k of the $n^{\rm th}$ time segment. In this case, S_k obeys the central limit theorem and, for sufficiently large $N_{\rm avg}$, is normally distributed with a variance that scales as $1/N_{\rm avg}$. Since $df = N_{\rm avg}/N_{\rm tc}\Delta t$, we see that there is a tradeoff between high frequency resolution and low variance of the spectral density. Because the lowest frequency of the spectrum (zero frequency excluded) is equal to df, the tradeoff is equivalently between a spectrum that extends low in frequency and one that is highly averaged.

To circumvent this tradeoff, we observe that, for our application, a high frequency resolution is not necessary at high frequencies. Similarly, at low frequencies we can tolerate relatively few averages, which in turn gives us high frequency resolution. This situation suggests that we compute an averaged FFT with relatively low $N_{\rm avg,min}$ for low frequencies and large $N_{\rm avg,max}$ for high frequencies. The spectra generated by using different values of $N_{\rm avg}$ can be stitched together at some intermediate frequency $f_{\rm cut}$. If $N_{\rm avg,min}$ and $N_{\rm avg,max}$ are significantly different, intermediate values of $N_{\rm avg}$ can be used as well. Our standard 1 hr time captures consist of $3200*1024 = 3,276,800$ points, sampled at 1024 Hz. To generate a spectrum, we use $N_{\rm avg} = [3, 12, 50, 200, 800, 3200]$ to generate 6 FFT's, which we stitch together at the frequencies $f_{\rm cut} = [1/2^{10}, 1/2^8, 1/2^6, 1/2^4, 1/2^2] * (512 \text{ Hz}/50) = [0.01, 0.04, 0.16, 0.64, 2.56]$.

[@@@ Show some figures?]

[@@@ Advantages when fitting?]

Bibliography

[1] F. C. Wellstood. *Excess Noise in the DC Squid; 4.2 K to 20 mK*. Ph.D. thesis, University of California, Berkeley (1988).

[2] K. K. Likharev and V. K. Semenov. "Fluctuation Spectrum in Superconducting Point Junctions." *Sov. Phys. JETP* **15**, 442 (1972).

[3] W. C. Stewart. "Current-voltage characteristics of josephson junctions." *Appl. Phys. Lett.* **12**, 277 (1968).

[4] D. E. McCumber. "Effect of ac impedance on dc voltage-current characteristics of superconductor weak-link junctions." *J. Appl. Phys.* **39**, 3113 (1968).

[5] H. Nyquist. "Thermal agitation of electric charge in conductors." *Phys. Rev.* **32**, 110 (1928).

[6] C. Tesche and J. Clarke. "dc squid: Noise and optimization." *J. Low Temp. Phys.* **29**, 301 (1977).